Ecological Modelling 273 (2014) 86–95

Contents lists available at ScienceDirect

Ecological Modelling

journal homepage: www.elsevier.com/locate/ecolmodel

Application of L-systems to geometrical construction of chamise and juniper shrubs

Dallan R. Prince, Marianne E. Fletcher, Chen Shen, Thomas H. Fletcher*

Chemical Engineering Department, Brigham Young University, Provo, UT 84602, United States

ARTICLE INFO

Article history:
Received 30 May 2013
Received in revised form 12 October 2013
Accepted 1 November 2013
Available online 30 November 2013

Keywords:
L-systems
Shrub geometry
Wildland fire

ABSTRACT

Improved models of fire spread and fire characteristics are desired for live shrub fuels, since the majority of existing research efforts focus on either dead fuel beds or crown fires in trees. Efforts have been made to improve live fuel modeling, including detailed studies of individual leaf combustion, with results incorporated into a shrub combustion model for broadleaf species. However, this approach was not well-suited to non-broadleaf shrubs since their fuel consists of long needle-covered branches rather than easily discretized leaves. Methods were therefore developed to simulate the branching structure of chamise (*Adenostoma fasciculatum*) and Utah juniper (*Juniperus osteosperma*). The plant structure was based on a form of fractal theory called Lindenmayer systems (i.e., L-systems). Correlations to predict branch number from crown diameter were made based on data from the literature, to ensure that the modeled shrubs would have the same bulk density as live shrubs. The structure model was designed to match the specific characteristics of each species, such as branching angles, the number of stems exiting at ground level, and the fuel element length. This method can be used to generate shrub geometries for detailed shrub combustion models or for realistic artistic renditions.

1. Introduction

A significant number of wildland fires in the western United States occur in areas with non-continuous groundcover comprised mostly of live shrubs. Current fire spread models used in the United States assume homogeneous fuel (Finney, 1998; Reinhardt et al., 2003; Scott and Burgan, 2005; Andrews, 2007) and are based on a semi-empirical surface spread model for dead fuels (Rothermel, 1972) with Van Wagner's crown fire ignition and propagation models (Van Wagner, 1976). However, natural fuel sources are neither completely dead nor homogeneous. It has been suggested that live fuels burn differently than dead fuels (Dimitrakopoulos, 2001; Zhou et al., 2005; Pickett, 2008; Prince and Fletcher, 2013a). Heterogeneous fuels have been shown to exhibit different combustion behavior than homogeneous fuels (Pimont et al., 2009; Parsons et al., 2011). Most of these models seem to underestimate the rate of spread compared to field data (Cruz and Alexander, 2010).

Several mechanistic physics-based computational fluid dynamics (CFD) models have been developed (Linn, 1997; Morvan and Dupuy, 2001; Linn et al., 2002, 2005; Dupuy and Morvan, 2005; Mell et al., 2007, 2009) which address fuel heterogeneity. These models have been used to simulate fires at scales as small as single-tree level, (Mell et al., 2009) thereby evaluating the effect that heterogeneity has within a single tree (Parsons et al., 2011). However, current landscape-scale models generally are limited to a grid dimension of about 2 m by 2 m by 2 m, averaging fuel behavior at the ground level.

Since CFD models require excessive computational power and time, simpler approaches to describe shrub combustion are being developed. For example, Pickett (Pickett, 2008; Cole et al., 2009) developed a semi-empirical shrub combustion model based on burning characteristics of individual leaves (Engstrom et al., 2004; Fletcher et al., 2007; Cole et al., 2011). In Pickett's model for broadleaf species, leaves were placed randomly in 2-dimensional space and fire spread was simulated through the domain. Leaves were assigned physical parameters (length, width, thickness, mass and moisture content) to which flame characteristics (ignition time, flame height, time of maximum flame height, and flame duration) were correlated. Flame width and flame interactions were also modeled. These characteristics define the flame location of a burning leaf over time. After exposure to another flame for their entire ignition time, leaves were ignited, and then followed their flame sequence to burn out. Fire propagated when flames from burning leaves overlapped unburned leaves, which ignited, and so on. Later models were expanded to three dimensions, and placed leaves randomly in locations similar to the overall bush shape (Prince and

* Corresponding author at: 350 CB, Chemical Engineering Department, Brigham Young University, Provo, UT 84602, United States. Tel.: +1 801 422 6236; fax: +1 801 422 0151.
E-mail address: tom_fletcher@byu.edu (T.H. Fletcher).

0304-3800/$ – see front matter © 2013 Elsevier B.V. All rights reserved.
http://dx.doi.org/10.1016/j.ecolmodel.2013.11.001

Fletcher, 2013b). However, for branching species, chamise (*Adenostoma fasciculatum*) and Utah juniper (*Juniperus osteosperma*), fuel is highly concentrated along the branching structure, so matching the stem structure is important. Furthermore, the complexity of spatial distribution within plants (Busing and Mailly, 2004) warrants the use of methods that provide more detail for the structure of branching species. There are many ways to simulate plant architecture (Godin, 2000). However, fractal theory presented the best match for the speed and simplicity of the shrub combustion model. A branching shrub defined by fractal theory provides locations and some physical description for fuel segments, which can be used with correlations for the flame characteristics to model fire spread in a model such as Pickett's.

Plants have been shown to follow fractal patterns (Alados et al., 1999; Godin et al., 2004), and fractals have been used to represent several aspects of plant geometry including tree crowns (Berezovskaya et al., 1997), leaf and branch properties (van Noordwijk and Mulia, 2002), roots (Fitter and Stickland, 1992; Ozier-Lafontaine et al., 1999; Richardson and Dohna, 2003), and entire plants (Yang and Midmore, 2009). Lindenmayer-systems (or L-systems), one method of applying fractals to plant structures, provides a simple way to generate and visualize a self-similar plant (Prusinkiewicz and Lindenmayer, 1990). L-systems are simple enough that they can be used to simulate plant structure effectively without requiring an extensive background in plant physiology (Renton et al., 2005), and the versatility of the approach enables it to be used for many different processes (Prusinkiewicz, 1997, 1998) such as modeling biomechanics in plant structure (Jirasek et al., 2000), simulating carbohydrates and carbon-allocation within trees (Allen et al., 2005), and transforming hand-drawn sketches into computer-simulated plants (Sun et al., 2008; Anastacio et al., 2009). Several models use L-systems along with other methods to model plant architecture (Salemaa and Sievänen, 2002; Renton et al., 2005; Pradal et al., 2009).

The objective of this work is to develop a method to accurately describe the distribution of fuel elements within chamise and Utah juniper shrubs. This method can be used with different types of shrub combustion models, ranging from mechanistic to empirical.

2. Methods

Live chamise and Utah juniper were measured and observed. Relevant data were collected from the literature, where available. These were used to develop correlations, and guided the development of L-systems-based models to describe the geometry and fuel placement of live shrubs.

2.1. Measurements, observations and correlations

Measurements were taken of eight live chamise shrubs in Southern California. Twenty-two Utah juniper shrubs were measured in Utah County, Utah. Additional details are described by Shen (2013).

2.2. Description of chamise

Chamise typically grows with multiple primary branches (or stems) emerging from the ground together (see Fig. 1). The mean basal circumference (around the emerging stems) was 184 ± 64 cm (95% confidence interval). The radius, assuming a circular branch placement, provided an estimate of the distance of each stem from the center of the group.

The branch length and branch tip height were used to determine the tilt angle from vertical (φ) of two primary branches from each shrub. The maximum measured primary branch angle (φ_{max}) was 77°. Secondary branch angles (δ) were determined for two secondary branches on each primary branch by measuring the length of the secondary branch (from its split with the primary branch) and the distance from the secondary tip to the primary branch. The length ratio (ε) of secondary branches to their parent primary branch was determined from the measured lengths of both. A total of 32 measurements were used to determine mean values and 95% confidence intervals for $\delta(30° \pm 6°)$ and $\varepsilon(0.45 \pm 0.06)$.

Fig. 1. A picture of a chamise shrub after the branches have been cut off showing that multiple primary branches emerge from the ground.

Segments with diameters of less than a quarter-inch (6.4 mm) were considered as the combustible fuels, so the distribution of thicknesses of segments less than a quarter-inch was studied in detail. Six-centimeter segments were cut from a chamise branch starting at the tips, and the thickness of each segment was recorded. Thicknesses were not uniformly distributed (see Fig. 2). The probability distribution for segment thickness is given in Eq. (1), where t is thickness (mm) and x is a random number between 0 and 1 assigned to each segment.

$$t = \frac{1}{x^{0.383}} \quad (1)$$

Measurements made by Countryman and Philpot (1970) were used to develop a correlation for predicting total mass, m_{tot}, from shrub height (Eq. (2)).

$$m_{tot} = 0.2868\, e^{1.201\, h} \quad (2)$$

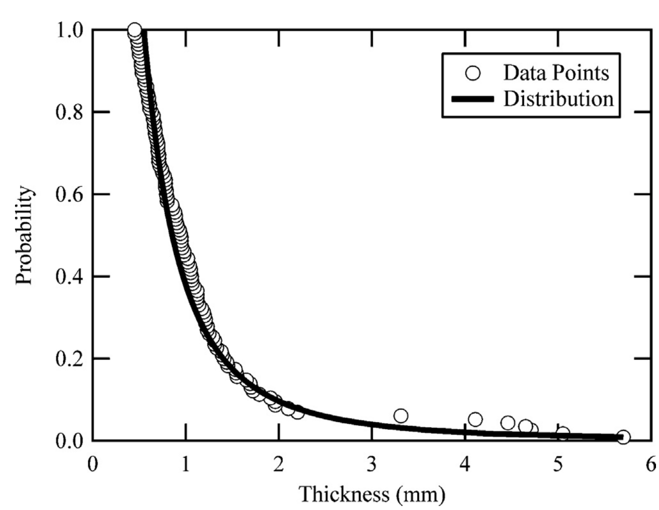

Fig. 2. Measured and modeled distribution of segment thicknesses for chamise.

Table 1
The coefficients for each size class (by diameter) used in Eq. (3).

Size class	a_1	a_2	R^2
0.25″	0.1729	0.1514	0.96
0.25″–0.5″	0.2141	−0.0073	0.95
0.5″–1″	0.3312	−0.0323	0.93
1″–3″	0.2092	−0.2081	0.81

Using the data of Countryman and Philpot (1970), a correlation was developed to predict the distribution of branch mass into four size classes. A fifth category for foliage (i.e. small needles) was also included in the original data, but in the correlation it was included in the combustible fuel class (quarter-inch or less). The amount of mass expected in each category, or size class, was correlated to the total fuel mass (Eq. (3) and Table 1).

$$m_{\text{cat},i} = a_1 m_{\text{tot}} + a_2 \quad (3)$$

A correlation for the wet mass of individual segments in the combustible fuel class is shown in Eq. (4), where t is thickness (mm), MC is leaf moisture content (dry basis), and l_f is segment length (cm).

$$m_i = -0.13575 + 0.136 \cdot t + 0.127 \cdot MC + 0.0178 \cdot l_f \quad (4)$$

2.2.1. Description of Utah juniper

Crown diameter (d_{crown}) was determined by averaging two different cross-sectional measurements taken at maximum crown diameter for twenty shrubs. Shrub height (h) was also measured and h was correlated to d_{crown} (Eq. (5) and Table 2). Short-biased and tall-biased correlations were also determined from 21 shrubs, which fall within the range of measurements but approximately follow the 25 and 75% quartiles of height.

$$\frac{h}{\text{cm}} = b_1 \left(\frac{d_{\text{crown}}}{\text{cm}} \right)^{b_2} \quad (5)$$

Near the base of the juniper trunk, primary branches frequently extended below horizontal but then curved upwards. Minimum primary branch angles typically occurred near the top of the shrub and the smallest measured branch angle (base-to-tip from vertical) was 17°. The top of a juniper extends vertically and if treated as a branch has an angle of approximately 0°.

Secondary branch angles were determined with the same method as was used for chamise and had a mean and 95% confidence interval of $\delta = 38.6° \pm 4.7°$ based on 29 measurements from 4 shrubs. The mean and 95% confidence interval of the length ratio of the highest to lowest primary branch was 0.48 ± 0.17 based on 6 shrubs. Foliage units, or fuel elements, were distributed along the exterior end of branches at a regular interval. The mean distance between fuel elements was 1.5 ± 0.10 cm (95% confidence interval) based on 79 measurements from 15 tertiary branches on 3 secondary branches.

Correlations for the dry mass of fuel were determined from measurements. Dry mass was estimated by sampling representative fuel units and then counted the number of units present on the shrub. The samples were oven-dried and weighed, and the dry mass of the entire juniper shrub was estimated based on 21 shrubs. Dry mass was correlated to crown diameter. Data from Mason and Hutchings (1967) was also used. Mason and Hutchings divided their measurements of Utah juniper shrubs into three different classifications – sparse, medium, and dense – and reported new growth foliage yields (including foliage and fruit). Yield was considered to be 30% of the total foliage and 50% of the total fruit. Therefore, to get the total dry mass of the shrub, their reported yield values were divided by 0.3, assuming that fruit yield was negligible. Correlations for m_{dry} for juniper are given by Eq. (6) and Table 3.

$$\frac{m_{\text{dry}}}{\text{kg}} = a_1 \left(\frac{d_{\text{crown}}}{\text{cm}} \right)^2 + a_2 \frac{d_{\text{crown}}}{\text{cm}} + a_3 \quad (6)$$

Table 2
The coefficients for h versus d_{crown} (Eq. (2)). Alternatively, h may be specified directly in the model.

Model	b_1	b_2	R^2
Short-biased	9.8	0.60	n/a
Average	21.067	0.4786	0.3480
Tall-biased	50	0.35	n/a

Table 3
The coefficients for correlations by Shen (2013) and Mason and Hutchings (1967) data used in Eq. (6).

Model	a_1	a_2	a_3	R^2
Shen	0.000	3.005×10^{-2}	−1.764	0.7104
M&H Sparse	2.506×10^{-5}	8.632×10^{-3}	-1.820×10^{-1}	0.9997
M&H Medium	5.478×10^{-5}	7.578×10^{-3}	-2.225×10^{-1}	1.0000
M&H Dense	7.979×10^{-5}	1.079×10^{-2}	-3.229×10^{-1}	1.0000

The R^2 for Shen's correlation is based on its fit to individual measurements, while the R^2 for Mason and Hutchings is for its fit to average measurements for all loam soil types.

2.3. Overview of models

Methods were developed to produce plant geometry similar to two branching species – chamise (*A. fasciculatum*) and Utah juniper (*J. osteosperma*). The models for these species follow the same general algorithm: (1) crown diameter is specified (and for juniper, models for shrub height and denseness are also specified); (2) a target mass is determined and used to specify the number of primary branches; (3) branch angles and starting locations are set; (4) branch geometry is determined by L-systems; (5) fuel physical parameters are specified (mass, dimensions, etc.); (6) shrub is either visualized or exported to a fire spread model. A model was designed and customized for each species to reflect their unique characteristics.

2.4. Chamise model

Symbols used to create strings in the chamise model included 'F' (forward one step of length d), '+' (left in x-plane by angle δ), '−' (right in x-plane by angle δ), '*' (left in y-plane by angle δ), '!' (right in y-plane by angle δ), and 'X' (string replaced with each derivation). The 'X' command was also implicitly interpreted as a new branch in the chamise model. Chamise branches exhibited complex branching behavior making it difficult to identify common patterns for L-systems strings. Consequently, the strings in the chamise model were treated as variables which allowed the user to vary the dry mass and bulk density of the shrub. Strings were chosen that produced a dry mass and bulk density that matched observed values.

There was no single string which could characterize the irregular shape of an entire branch. For this reason a stochastic element was added. An equal probability was assigned for choosing any one of several strings. Each derivation was randomly assigned one string, so branches were similar but not identical. Strings used in the chamise L-systems model were: (1) F + !XF + *X − *XFFF − !XXF; (2) F!X* − XF + *X! − XFFF + XX; (3) F − *X − !XFFF − XFF + *XXFF; (4) F − *XF + XFF + !X!XFF + *XX; and (5) F!X + XFFF*X! − XFFFX.

To generate the geometry of an entire shrub, multiple stochastic, three-dimensional branches were combined and became the primary branches of the shrub. The number of primary branches, κ, in the shrub was based on experimental data. The primary branch lengths and angle measurements for live shrubs were used in the

Table 4
L-systems rules governing symbol interpretation for Utah juniper according to string location.

Symbol location	Step length (cm)			Turn/pitch/roll angle (degrees)	Application
	F	H	S		
1, 2	22	–	–	–	First primary branch segment
3, 4	11	–	–	$10–10i_b/\kappa$	Second primary branch segment
>4	–	1.5	3	38.4	All foliage-related branching

'F' length is scaled from the given value to achieve the specified shrub diameter and conical shape.

Table 5
L-systems rules governing symbol replacements for Utah juniper.

Before	After (symbol replacement rules)				
	Set A	Set B	Set C	Set D	Set E
F	F	F	F	F	F
G	G	G	HH[/+G]HH[−G]HH[&\G]H or HH[/+G]HHHH[&\G]H	HHHHHHH	Undefined
X	F[&X[G]]	G	Undefined	Undefined	Undefined
H	Undefined	Undefined	H	H	H[/+S] or H[\−S]
S	Undefined	Undefined	Undefined	Undefined	S
Derivation	1, 2	3	4, 5	6	7
Result	Grow primary branches F; begin foliage-branch starts	Complete foliage-branch starts G	Grow foliage branches from starts H	Complete foliage branches H	Add foliage segment S to foliage branch segments H

The derivation(s) when each rule is active and its anatomical result are also summarized.

model. Each branch was assigned angles of rotation about the *z*-axis (θ) and tilt from vertical (φ) so that the primary branches evenly divided the three-dimensional space (see Fig. 3). An additional variable was also added to non-uniformly specify the radius of a starting branch from the center point of the shrub. The φ values were determined from a normal distribution with a user-specified standard deviation and mean, and the θ values were determined from a normal distribution using a mean of:

$$\mu_\theta = \frac{360^\circ}{\kappa} \quad (7)$$

The θ values were then added together consecutively so that the angles got progressively larger:

$$\theta_i = \theta_{i-1} + \mu_\theta \quad (8)$$

In using different strings the length of the branch would be dependent on the number of 'F's in the current string instead of on the length of the branch. To avoid this problem, the equation for finding the length of one 'F' was normalized according to the total number of 'F's in the current string (n_F) (Eq. (9)). The length for the first derivation (d_0) and the ratio (ε), which is the ratio of the length of the second derivation to the length of the first derivation, were also used. An option was included to calculate d_0 using a normal distribution with a user-specified standard deviation. The height of the shrub, *h*, was calculated using the primary branch length and the scaling factor (Eq. (10)).

$$d = \frac{d_0 \cdot \varepsilon^{n_i - 1}}{n_F} \quad (9)$$

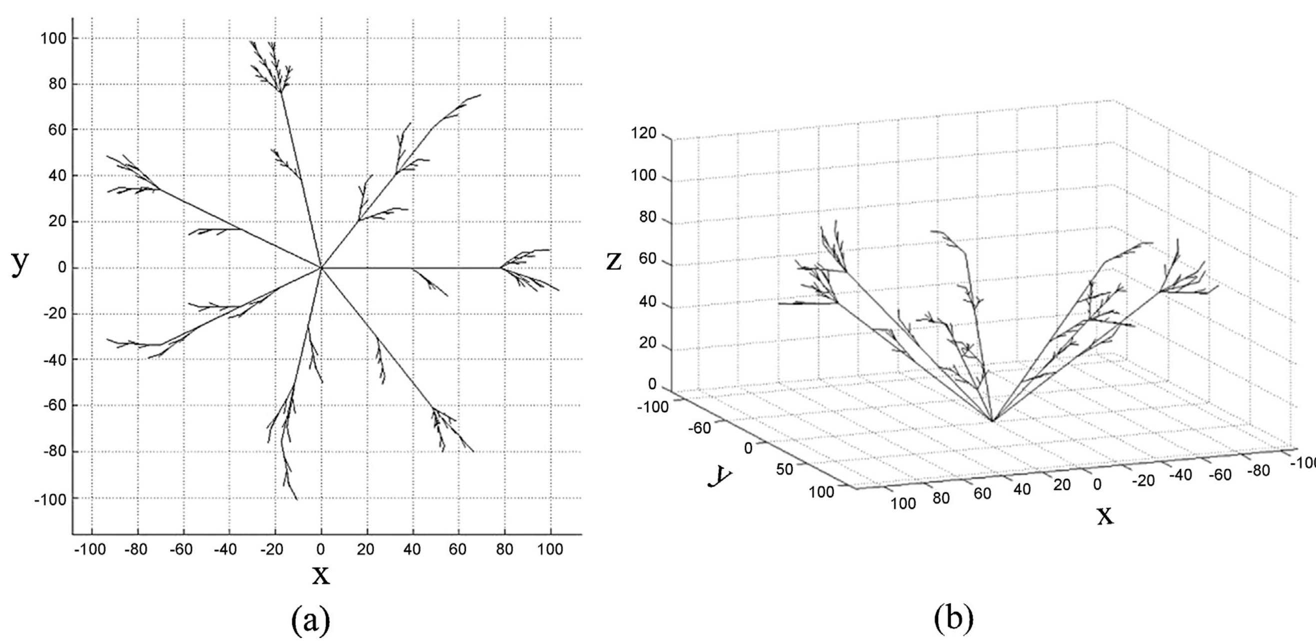

Fig. 3. An example of a plant with seven primary branches to illustrate how the values of (a) φ and (b) θ evenly divide the three-dimensional space.

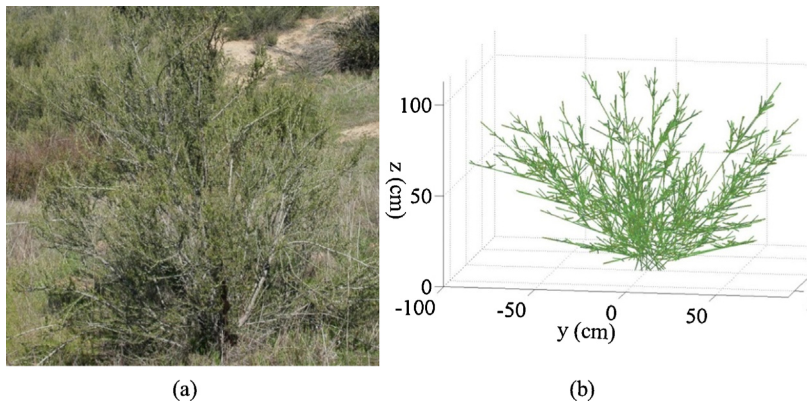

Fig. 4. A visual comparison of (a) a chamise shrub (b) and an example of a modeled chamise shrub.

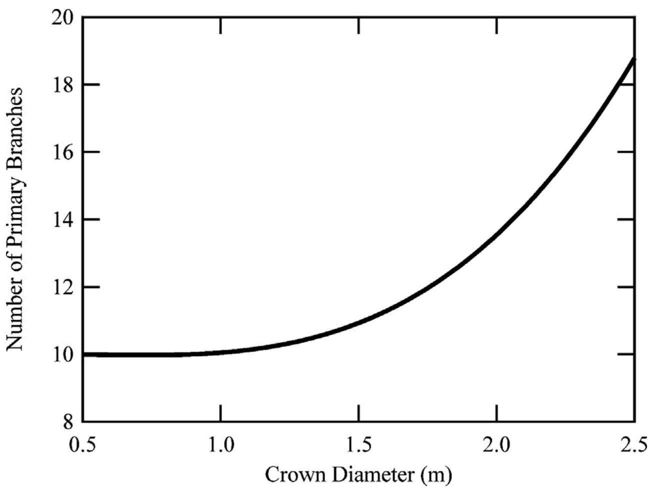

Fig. 5. This graph shows the relationship between crown diameter and the number of primary branches for a chamise shrub.

$$h = d_0 + \varepsilon \cdot d_0 \quad (10)$$

The chamise model also split the branches into smaller segments with a length (l_f) defined by the user. Using Eq. (3), based on data from Countryman and Philpot (1970), the number of fuel segments in each fuel thickness class was prescribed. Each branch segment was assigned to a thickness class according to its radius from the origin, where a larger radius corresponds to a smaller segment diameter.

Individual segment thicknesses (within each class) were also assigned based on the distance of the segment from the origin. Segments with a thickness less than a quarter-inch were considered fuel elements or the segments most likely to burn. The individual wet masses of fuel elements were assigned using Eq. (4). Masses were then assigned to all other segments by calculating their cylindrical volumes and multiplying by the density of wood.

The branch segment masses (for the given l_f and each diameter) and the prescribed mass of each size class were used to determine the number of segments in each class. Based on l_f and the primary branch length, the number of segments required to complete each primary branch was estimated. The number of primary branches was then determined by dividing the total number of segments by the number of segments per primary branch.

2.5. Utah juniper model

The diameter, a dry mass correlation, and a height correlation were first selected. Height and dry mass models affect bulk density, which can account for the effect of environmental factors (such as

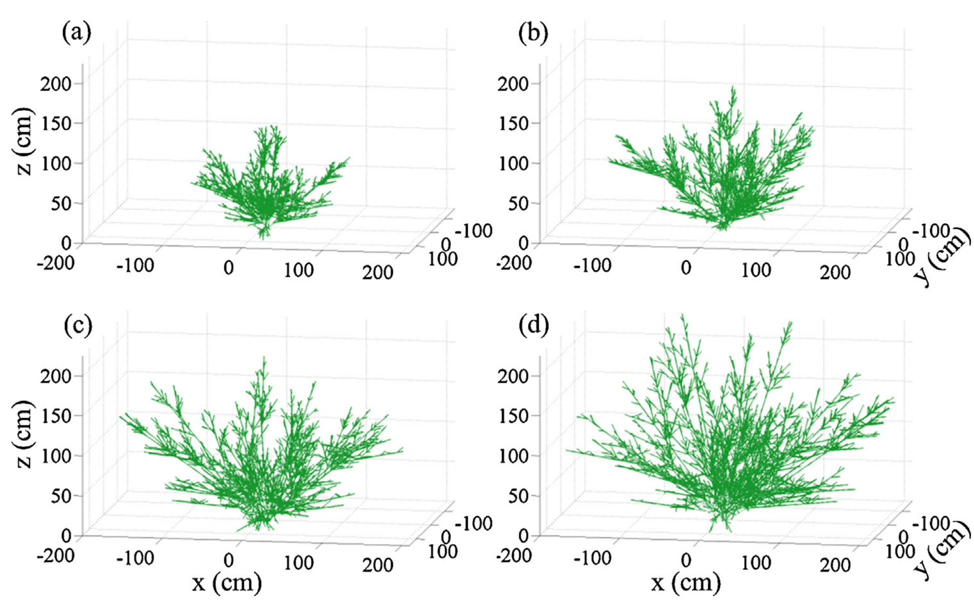

Fig. 6. Chamise shrubs generated based on crown diameter. (a) 300 cm crown diameter with 98 primary branches, (b) 350 cm crown diameter with 117 branches, (c) 400 cm crown diameter with 139 branches, and (d) 450 cm crown diameter with 166 primary branches.

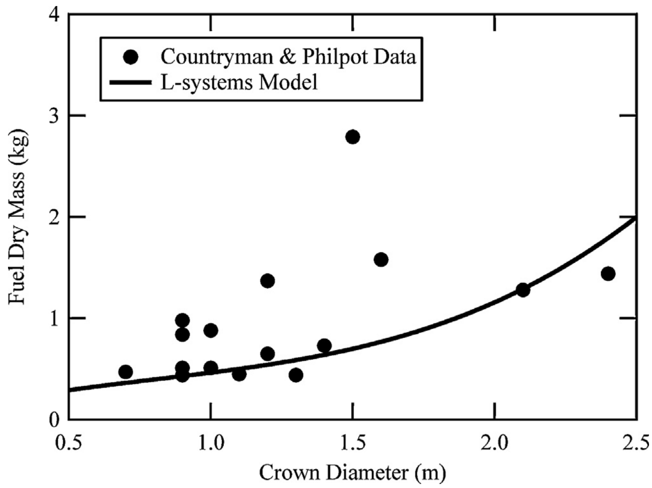

Fig. 7. Results from the L-systems model compared to the data from Countryman and Philpot (1970) for chamise. "Fuel" in the model was defined as all segments with a thickness less than a quarter inch.

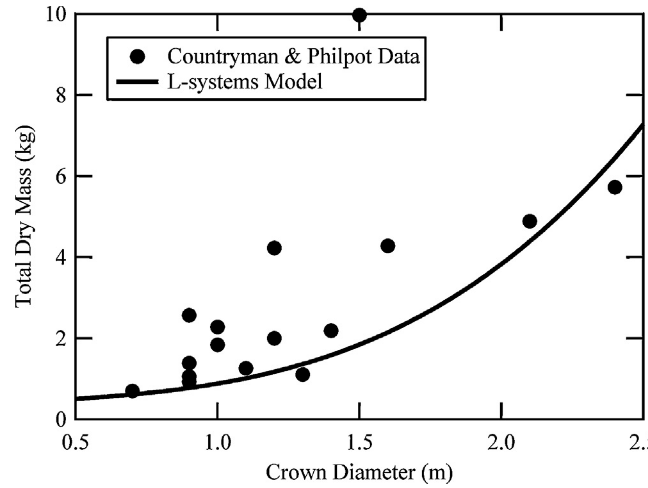

Fig. 8. Total predicted and measured shrub mass as a function of crown diameter for chamise.

soil quality and sunlight) on foliage production. The resulting m_{dry} was divided by the average dry mass per branch to prescribe κ.

Branches were evenly spaced along the trunk to reach the shrub height specified by the height correlation and were numbered from bottom to top. To imitate natural primary branching angles in the model φ was set to decrease with increasing branch number (i_b) (see Eq. (11)). This nominally results in a φ of 30° (taken at the trunk) for the top branch, but due to branch curvature, its effective angle (from base-to-tip) was near 0°. The behavior of Eq. (11) reserved most of the change in angle to the top branches, which had shorter segments without foliage. This helped to distribute foliage more evenly in the shrub. Random variation (υ) was included which was a random angle pulled from a normal distribution (standard deviation of 3°).

$$\varphi = 100 - 35\left(\frac{i_b}{\kappa}\right) - 35\left(\frac{i_b}{\kappa}\right)^6 + \upsilon \qquad (11)$$

The bend in each primary branch was reduced with increasing i_b, although the curvature in the foliage-laden branches was left unchanged (see Table 4). A secondary branch angle of 38.4° was selected from the 95% confidence interval of measurements for live shrubs. To achieve the measured branch length ratio of 0.48 ± 0.17, the top branch was made about half as long as the bottom branch; the non-foliage-laden section of the branch was scaled from being approximately half the branch at the bottom to nearly zero at the top, while the foliage-laden section remained constant. Fuel elements (i.e. foliage units) were placed at the average measured interval along foliage-laden sections.

Each branch was specified using L-systems. Symbols included capital letters (step forward), '+' (turn left), '−' (turn right), '&' (pitch down), '^' (pitch up), '\' (roll left), '/' (roll right), '[' (start a new branch), and ']' (recall last position before branching). Symbols were compiled and interpreted using a script developed based on an L-systems program available from Land (2006). Five sets of rules were used to govern symbol replacements and were assigned to particular derivations, as detailed in Table 5. Where multiple strings were provided for the same replacement, each was given an equal probability of being used. This approach produced stochastic strings which were similar but not identical. Strings were interpreted to reflect the measurements and observations of live juniper shrubs, as detailed in Table 4. The 'F' step was scaled from the length given in the table to achieve the intended shrub diameter and conical shape. The starting seed 'X' was used with a starting direction of $(x, y, z) = (0, 0, 1)$.

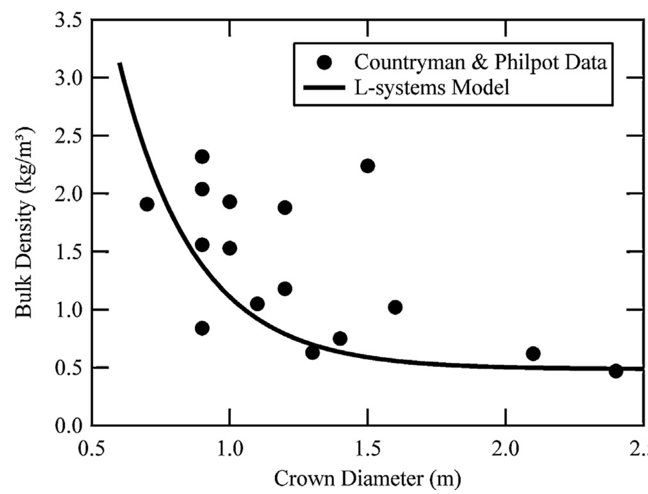

Fig. 9. Predicted and measured bulk density of chamise as a function of crown diameter for chamise.

Each completed branch was (1) rotated to its assigned φ (Eq. (11)), (2) translated to its intended height on the juniper trunk, and (3) rotated about the trunk. The rotation about the trunk was somewhat randomized but also favored a non-overlapping radial distribution.

3. Results and discussion

3.1. Chamise

Visually, the model generated shrubs that look similar to young chamise shrubs (see Fig. 4). The basic overall shape was a hemisphere, with the distribution of primary branches filling the complete space. Table 6 also shows that the physical measurements of both shrubs shown in Fig. 4 are very similar as well.

Table 6
Measurements of the chamise shrub in Fig. 4(a) versus the modeled shrub in Fig. 4(b).

Measurement	Measured	Calculated
Crown diameter (cm)	140	140
Number of primary branches	14	12
Dry mass (g)	494 (predicted)	482

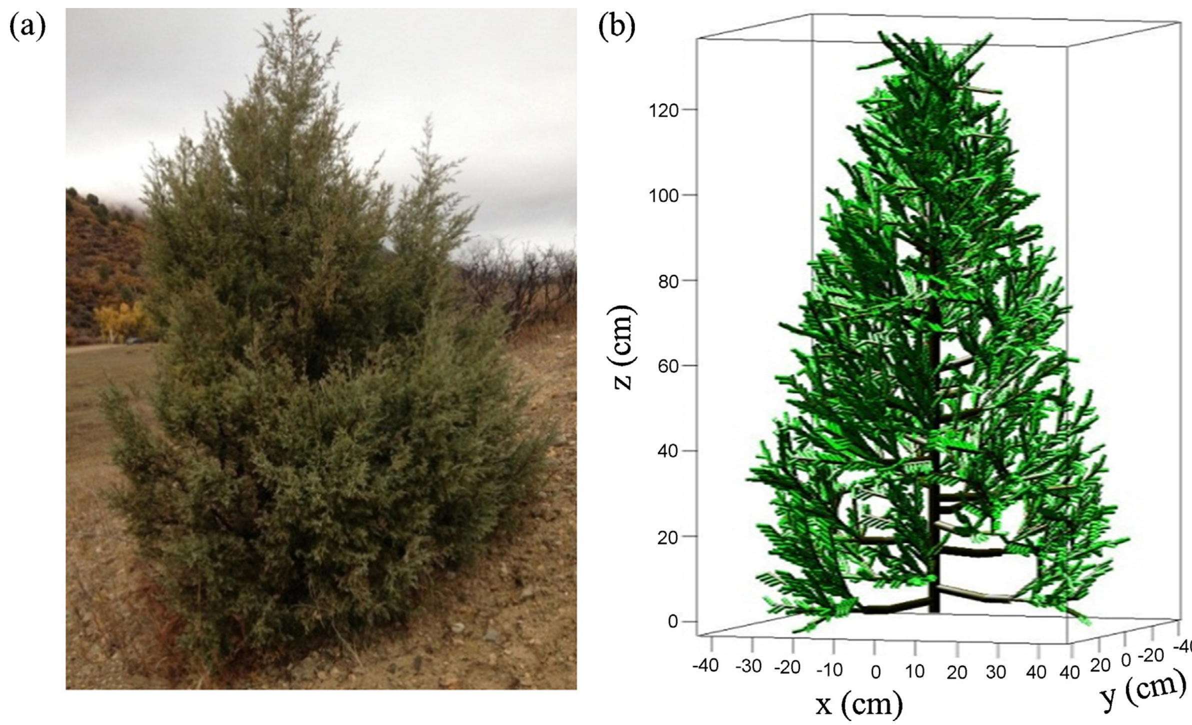

Fig. 10. Visual comparison of (a) a Utah juniper shrub and (b) a shrub geometry generated by the L-systems approach having 35 branches.

The crown diameter measured for the shrub in Fig. 4(a) was input into the model to generate the shrub in Fig. 4(b). The other two measurements, average primary branch radius from the center of the shrub and number of primary branches, were calculated by the model. The dry mass shown in Table 6 in the "measured" column was predicted by the correlations in Eqs. (2) and (4).

As mentioned previously, the number of primary branches per shrub was calculated based on the crown diameter of the shrub. This calculation eliminates the necessity of the user having to know how many primary branches should be on the shrub, and ensures that the bulk density of the shrub is in the correct range. Fig. 5 is a graph illustrating how crown diameter influences the number of primary branches. Fig. 6 shows a comparison of modeled chamise shrubs with different crown diameters. These diameters extend beyond those presented in Fig. 5 but the number of primary branches was calculated in the same way. However, for shrubs that large, it is likely that some of the modeled primary branches would actually be members of the same shoot emerging from the ground, thereby reducing the total count of primary branches (see Fig. 6).

The dry mass of fuel elements was compared with data from Countryman and Philpot (1970). Fig. 7 shows the mass of fuel elements versus crown diameter for data from Countryman and Philpot and the results from the model. The model appears consistent with the data, although the model appears slightly low.

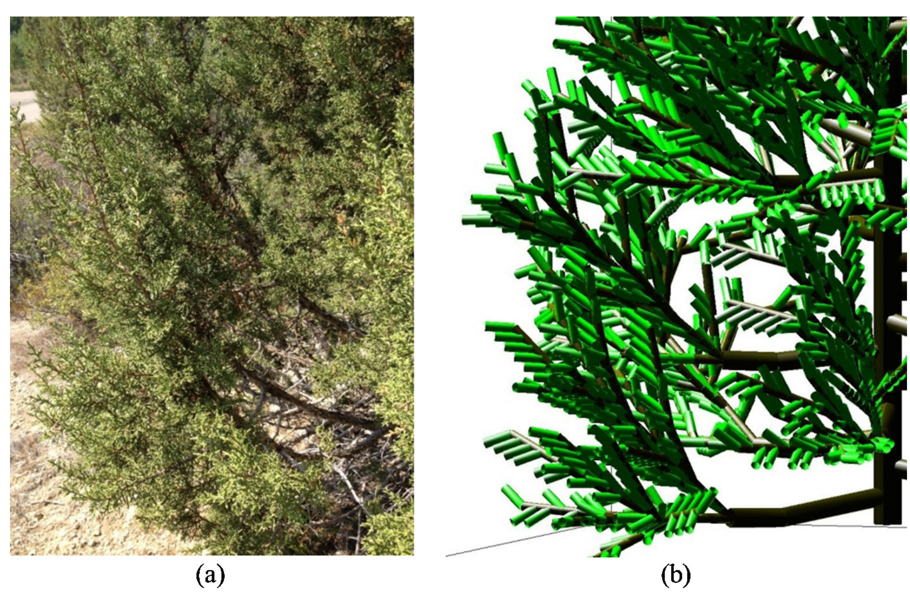

Fig. 11. (a) A close-up of the Utah juniper shrub and (b) a close-up of a modeled juniper.

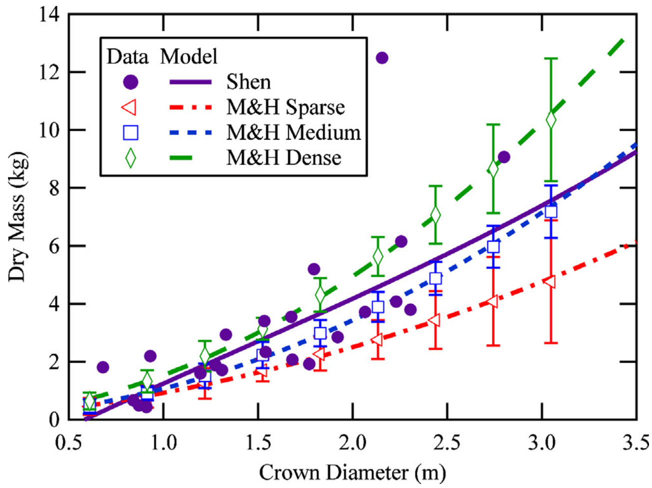

Fig. 12. Dry mass data (individual measurements from Shen and mean ± 2 standard deviations for Mason and Hutchings, 1967) and dry mass of modeled Utah juniper shrubs using each dry mass correlation for various crown diameters.

The sum of the masses of all segments gave the total shrub mass. The modeled total dry mass versus Countryman and Philpot (1970) data are shown in Fig. 8. Again, the model appears consistent with the data, but slightly low.

The volume of the shrub was also approximated by dividing the shrub into small, cubic sections and finding the fraction of boxes occupied by fuel. The estimated total volume was the cumulative volume of all boxes with fuel. Then, from the total shrub mass and volume, the bulk density was calculated, which is sometimes termed crown bulk density. The number of segments as well as the volume of the shrub is dependent on the crown diameter, so Fig. 9 is a graph of the bulk density versus the crown diameter. The model predictions are consistent with the data, but seem slightly lower than the average at any specific crown diameter.

Table 7
A comparison of the measurements of the shrub and the modeled shrub shown in Fig. 10.

Measurement	Measured	Modeled
Height (cm)	140	136
Crown diameter (cm)	84	90
Dry mass (g)	664	723

3.2. *Utah juniper*

The geometry for modeled Utah juniper is also visually similar to live shrubs. Fig. 10 shows a picture of a live shrub along with a modeled shrub. The crown diameter of the shrub in the photo was measured, and the model was given the same input. The fuel density of the shrub in the photo was estimated as being between sparse and medium. The modeled shrub was assigned 35 branches, which falls within this range. Table 7 shows a comparison between the dimensions of the shrub and the model in Fig. 10. The dimensions of the modeled shrub as well as the overall shape are very similar to the live shrub. The predicted height and crown diameter closely match, and the combustible dry mass generated by the model is within 9% of the estimated mass of the shrub in the picture.

In addition to matching the overall shape of the shrub, another focus of the model was to imitate the placement of fuel elements. Fig. 11 shows a closer view of one of the branches from the shrub in Fig. 10 along with examples of branches from the model. The branch curvature and fuel placement are similar. Each terminal cylinder represents one tiny foliage unit (or fuel element) having a mass of 0.102 ± 0.083 g (two standard deviations). The complex branched geometry of the foliage units was not represented.

The Mason and Hutchings (1967) m_{dry} versus d_{crown} data (collected in Cache County, Utah) with two-standard-deviation error bars is compared to the L-systems model predictions in Fig. 12. Shen's (2013) data (collected in Utah County, Utah) and its model predictions are also compared. In general the correlation from Shen (2013) fell between the medium and dense correlations

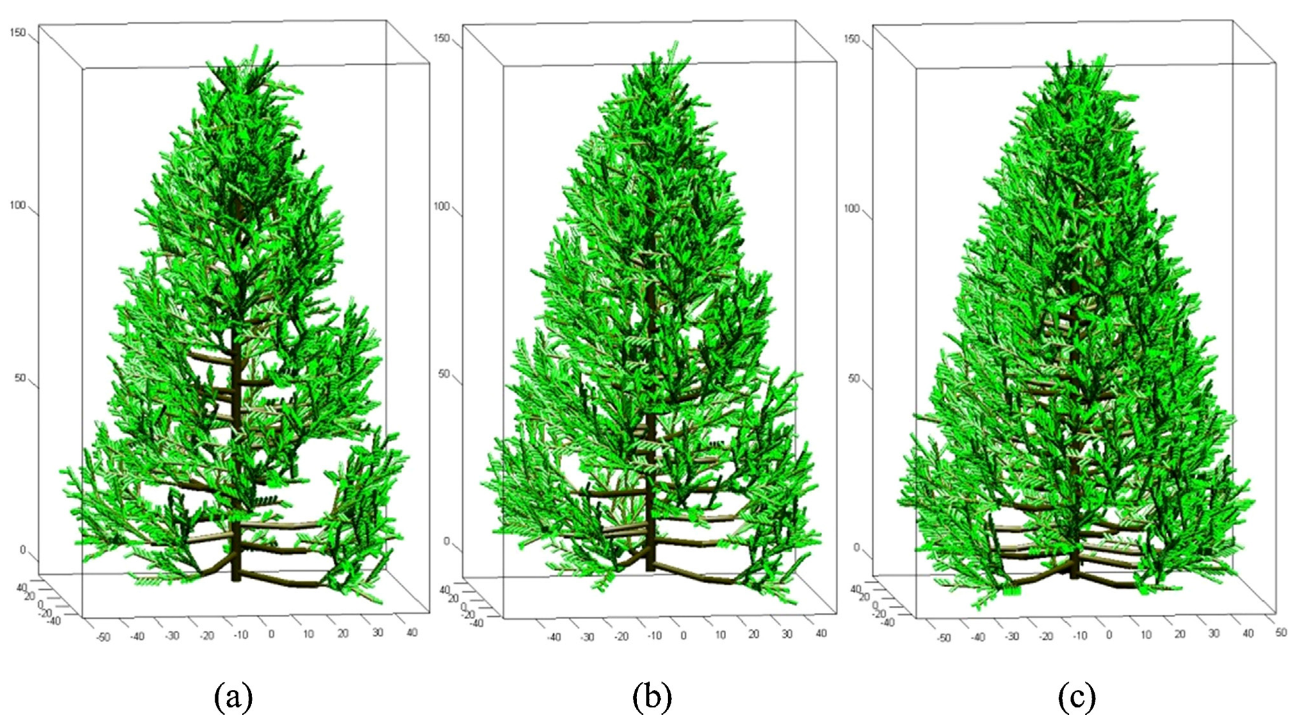

Fig. 13. Juniper shrubs generated for three classifications of fuel denseness with 1.0 m diameters and 1.6 m heights: (a) sparse with 76 branches; (b), medium with 106 branches; and (c) dense with 152 branches.

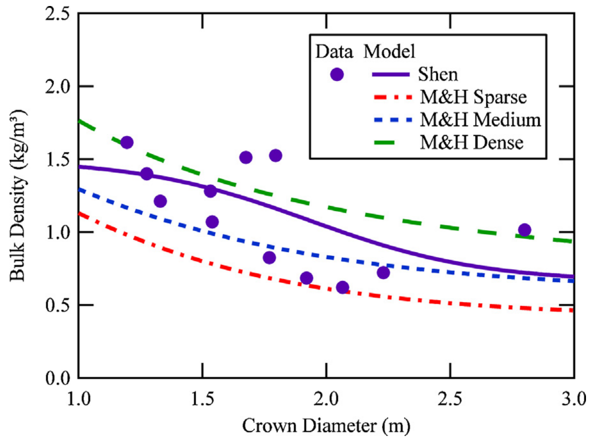

Fig. 14. Utah juniper bulk density data from Shen and bulk density of modeled juniper shrubs using each dry mass correlation (see Eq. (6)) for various crown diameters.

derived from data reported by Mason and Hutchings. The agreement between the two correlations strengthens the credibility of both. Shrubs using the three denseness classes of Mason and Hutchings are shown in Fig. 13. The effect of denseness is clearly reflected in the appearance of the shrubs. As with chamise, for larger juniper shrubs some of the modeled primary branches would actually be members of the same branch in a real shrub (Fig. 13).

The effect of crown diameter on bulk density was also compared between modeled shrubs using the different correlations, seen in Fig. 14. Bulk density was determined in the model by dividing the total dry mass by the total volume. The total dry mass equaled the sum of the individual masses of all fuel elements. The total volume was determined from the convex hull of the shrub. In the data presented from Shen (2013), dry mass was determined as previously described and volume was determined based on a cone stacked on a cylinder, with diameters equal to the measurements and respective heights of 75 and 25% the total height.

The influence of crown diameter on bulk density is particularly interesting in this case because crown diameter significantly impacts both the mass and the volume of the shrub. Crown diameter directly affects the shrub's dry mass. It is also affects volume because it is correlated to the height of the shrub and influences the crown diameter at every height. Hence, as crown diameter increases, both mass and volume also increase. The decrease in bulk density versus crown diameter is due to the fact that the modeled fuel mass is approximately related to the first or second power of diameter (see Eq. (6)) and volume is approximately related to the cube of the diameter.

4. Summary and conclusion

In order to accurately model the characteristics of each species, geometrical measurements were taken of chamise and juniper species, including number of primary branches, branch lengths and angles. Correlations were developed to describe stem diameter, mass, height, and crown diameter for these species.

Concepts from L-systems theory were incorporated into a model to generate branching shrub geometries specifically for chamise and Utah juniper. L-systems provided the basic framework for individual branch structure, and then several L-systems branches were combined to generate a shrub. The branches were assigned angles so that the overall shape of the shrub would imitate the structure of a real shrub. Additional customizations were added to better match specific characteristics of the individual species. In the chamise model, for example, a variable was added to replicate the characteristic of primary branches exiting the ground close together, but not from one central point. The Utah juniper model also included several customizations, such as having the primary branches emerge from various heights along the trunk of the shrub. Another enhancement to the basic L-system structure in the Utah juniper code included setting the string replacement rules to differ between derivations to simulate the complex structure of juniper branches. Furthermore, lengths and angles were manipulated according to symbol position (in the final string) and branch number (which was a surrogate for vertical position). The juniper customizations resulted in (1) evenly-spaced foliage, (2) primary branches which mimicked the curvature of natural branches and (3) a branching structure reflecting that of real branches.

The chamise and Utah juniper models visually imitate the shrub shapes of their respective species, and also match dry mass and bulk density data from literature and supplemental measurements. These characteristics make the chamise and Utah juniper models ideal for generating fuel structures for wildland fire models that require a detailed fuel description.

Acknowledgements

This research was funded in part by the Joint Fire Sciences Program (JFSP) and National Science Foundation Grant CBET-0932842. Any opinions, findings, and conclusions or recommendations expressed in this paper are those of the PI and do not necessarily reflect the views of the National Science Foundation; NSF has not approved or endorsed its content. Special thanks go to Joey Chong for the measurement, collection and shipping of live samples from California to Brigham Young University. Thanks also to Ganesh Bhattari, Jay Liu, Kristen Nicholes and Kenneth Alford for their valuable input.

References

Alados, C.L., Escos, J., Emlen, J.M., Freeman, D.C., 1999. Characterization of branch complexity by fractal analyses. Int. J. Plant Sci. 160, S147–S155.

Allen, M.T., Prusinkiewicz, P., DeJong, T.M., 2005. Using L-systems for modeling source-sink interactions, architecture and physiology of growing trees: the L-PEACH model. New Phytol. 166, 869–880.

Anastacio, F., Prusinkiewicz, P., Sousa, M.C., 2009. Sketch-based parameterization of L-systems using illustration-inspired construction lines and depth modulation. Comput. Graph. 33, 440–451.

Andrews, P.L., 2007. BehavePLUS fire modeling system: past, present, and future. In: Proceedings of the 7th Symposium on Fire and Forest Meteorology, Bar Harbor, Maine.

Berezovskaya, F.S., Karev, G.P., Kisliuk, O.S., Khlebopros, R.G., Tsel'niker, Y.L., 1997. A fractal approach to computer-analytical modelling of tree crowns. Trees, 323–327.

Busing, R.T., Mailly, D., 2004. Advances in spatial, individual-based modelling of forest dynamics. J. Veg. Sci., 831–842.

Cole, W.J., Pickett, B.M., Fletcher, T.H., Weise, D.R., 2009. A semi-empirical multi-leaf model for fire spread through a manzanita shrub. In: 6th U.S. National Combustion Meeting, Ann Arbor, Michigan.

Cole, W.J., Dennis, M.H., Fletcher, T.H., Weise, D.R., 2011. The effects of wind on the flame characteristics of individual leaves. Int. J. Wildland Fire 2011, 657–667.

Countryman, C.M., Philpot, C.W., 1970. Physical Characteristics of Chamise as a Wildland Fuel. USDA Forest Service, Berkeley, CA, Research Paper, PSW-66. 16 pp.

Cruz, M.G., Alexander, M.E., 2010. Assessing crown fire potential in coniferous forests of western North America: a critique of current approaches and recent simulation studies. Int. J. Wildland Fire 19, 377–398.

Dimitrakopoulos, A.P., 2001. Thermogravimetric analysis of Mediterranean plant species. J. Anal. Appl. Pyrolysis 60, 123–130.

Dupuy, J.L., Morvan, D., 2005. Numerical study of a crown fire spreading toward a fuel break using a multiphase physical model. Int. J. Wildland Fire 14, 141–151.

Engstrom, J.D., Butler, J.K., Smith, S.G., Baxter, L.L., Fletcher, T.H., Weise, D.R., 2004. Ignition behavior of live California chaparral leaves. Combust. Sci. Technol. 176, 1577–1591.

Finney, M.A., 1998. FARSITE: fire area simulator – model development and evaluation. In: USDA Forest Service Rocky Mountain Forest and Range Experiment Station Research Paper, 1-+.

Fitter, A.H., Stickland, T.R., 1992. Fractal characterization of root-system architecture. Funct. Ecol. 6, 632–635.

Fletcher, T.H., Pickett, B.M., Smith, S.G., Spittle, G.S., Woodhouse, M.M., Haake, E., Weise, D.R., 2007. Effects of moisture on ignition behavior of moist California chaparral and Utah leaves. Combust. Sci. Technol. 179, 1183–1203.

Godin, C., 2000. Representing and encoding plant architecture: a review. Ann. For. Sci. 57, 413–438.

Godin, C., Puech, O., Boudon, F., Sinoquet, H., 2004. Space occupation by tree crowns obeys fractal laws: evidence from 3D digitized plants. In: Godin, C. (Ed.), 4th International Workshop on Functional-Structural Plant Models. Motpellier, France, pp. 79–83.

Jirasek, C., Prusinkiewicz, P., Moulia, B., 2000. Integrating biomechanics into developmental plant models expressed using L-systems. In: Spatz, H.-C., Speck, T. (Eds.), 3rd Plant Biomechanics Conference. Plant Biomechanics, Freiburg-Badenweiler, pp. 615–624.

Land, B., 2006. BioNB 441, L-Systems in Matlab. Cornell University, Ithaca, NY https://instruct1.cit.cornell.edu/courses/bionb441/LSystem/

Linn, R.R., 1997. A transport model for prediction of wildfire behavior. PhD Thesis, Mechanical Engineering, New Mexico State Univ., Las Cruces, NM 212 pp.

Linn, R., Reisner, J., Colman, J.J., Winterkamp, J., 2002. Studying wildfire behavior using FIRETEC. Int. J. Wildland Fire 11, 233–246.

Linn, R., Winterkamp, J., Colman, J.J., Edminster, C., Bailey, J.D., 2005. Modeling interactions between fire and atmosphere in discrete element fuel beds. Int. J. Wildland Fire 14, 37–48.

Mason, L.R., Hutchings, S.S., 1967. Estimating foliage yields on Utah juniper from measurements of crown diameter. J. Range Manage. 20, 161–166.

Mell, W., Jenkins, M.A., Gould, J., Cheney, P., 2007. A physics-based approach to modelling grassland fires. Int. J. Wildland Fire 16, 1–22.

Mell, W., Maranghides, A., McDermott, R., Manzello, S.L., 2009. Numerical simulation and experiments of burning douglas fir trees. Combust. Flame 156, 2023–2041.

Morvan, D., Dupuy, J.L., 2001. Modeling of fire spread through a forest fuel bed using a multiphase formulation. Combust. Flame 127, 1981–1994.

Ozier-Lafontaine, H., Lecompte, F., Sillon, J.F., 1999. Fractal analysis of the root architecture of *Gliricidia sepium* for the spatial prediction of root branching, size and mass: model development and evaluation in agroforestry. Plant Soil 209, 167–180.

Parsons, R.A., Mell, W.E., McCauley, P., 2011. Linking 3D spatial models of fuels and fire: effects of spatial heterogeneity on fire behavior. Ecol. Model. 222, 679–691.

Pickett, B.M., 2008. Effects of moisture on combustion of live wildland forest fuels. Ph.D. thesis, Chemical Engineering, Brigham Young University, Provo, UT, 208 pp.

Pimont, F., Dupuy, J.L., Caraglio, Y., Morvan, D., 2009. Effect of vegetation heterogeneity on radiative transfer in forest fires. Int. J. Wildland Fire 18, 536–553.

Pradal, C., Boudon, F., Nouguier, C., Chopard, J., Godin, C., 2009. PlantGL: a Python-based geometric library for 3D plant modelling at different scales. Graph. Models 71, 1–21.

Prince, D.R., Fletcher, T.H., 2013a. A combined experimental and theoretical study of the combustion of live vs. dead leaves. In: 8th US National Combustion Meeting of the Combustion Institute, Park City, UT.

Prince, D.R., Fletcher, T.H., 2013b. Semi-empirical fire spread simulator for Manzanita, Utah Juniper and chamise shrubs. In: 8th US National Combustion Meeting, The Combustion Institute, Park City, UT.

Prusinkiewicz, P., 1997. A look at the visual modeling of plants using L-systems. In: Hofestädt, R., Lengauer, T., Löffler, M., Schomburg, D. (Eds.), Bioinformatics, vol. 1278. Springer, Berlin/Heidelberg, pp. 11–29.

Prusinkiewicz, P., 1998. Modeling of spatial structure and development of plants: a review. Sci. Hort. 74, 113–149.

Prusinkiewicz, P., Lindenmayer, A., 1990. The Algorithmic Beauty of Plants. Springer-Verlag, New York.

Reinhardt, E.D., Crookston, N.L., Beukema, S.J., Kurz, W.A., Greenough, J.A., Robinson, D.C.E., Lutes, D.C., 2003. The Fire and Fuels Extension to the Forest Vegetation Simulator. U.S. Department of Agriculture, Forest Service, Rocky Mountain Research Station, Ogden, UT, Document Number RMRS-GTR-116.

Renton, M., Kaitaniemi, P., Hanan, J., 2005. Functional-structural plant modelling using a combination of architectural analysis, L-systems and a canonical model of function. Ecol. Model. 184, 277–298.

Richardson, A.D., Dohna, H.Z., 2003. Predicting root biomass from branching patterns of Douglas-fir root systems. Oikos 100, 96–104.

Rothermel, R.C., 1972. A Mathematical Model for Predicting Fire Spread in Wildland Fuels. U.S. Department of Agriculture, Forest Service, Intermountain Forest and Range Experiment Station, Ogden, UT, pp. 40, Res. Pap. INT-115.

Salemaa, M., Sievänen, R., 2002. The effect of apical dominance on the branching architecture of *Arctostaphylos uva-ursi* in four contrasting environments. Flora 197, 429–442.

Scott, J.H., Burgan, R.E., 2005. Standard Fire Behavior Fuel Models: A Comprehensive Set for Use with Rothermel's Surface Fire Spread Model. United States Department of Agriculture, F.S., Fort Collins.

Shen, C., 2013. Application of fuel element combustion properties to a semi-empirical flame propagation model for live wildland Utah shrubs. M.S. thesis, Chemical Engineering Department, Brigham Young University, Provo, UT, 98 pp.

Sun, B., Jiang, L., Sun, B., Jiang, S., 2008. Research of plant growth model based on the combination of L-system and sketch. In: 9th International Conference for Young Computer Scientists, ICYCS 2008, 18 November 2008–21 November 2008. Inst. of Elec. and Elec. Eng. Computer Society, Zhang Jia Jie, Hunan, China, pp. 2968–2972.

van Noordwijk, M., Mulia, R., 2002. Functional branch analysis as tool for fractal scaling above- and belowground trees for their additive and non-additive properties. Ecol. Model. 149, 41–51.

Van Wagner, C.E., 1976. Conditions for the start and spread of crown fire. Can. J. For. Res. 7, 23–24.

Yang, Z.J., Midmore, D.J., 2009. Self-organisation at the whole-plant level: a modelling study. Funct. Plant Biol. 36, 56–65.

Zhou, X., Mahalingam, S., Weise, D., 2005. Modeling of marginal burning state of fire spread in live chaparral shrub fuel bed. Combust. Flame 143, 183–198.